Archive of Applied Mechanics (2024) 94:21–37
https://doi.org/10.1007/s00419-023-02498-x

ORIGINAL

Zheng Li · Zhidan Li · Yunsen Zhang · Daihai Chen · Shizhan Xu · Yu Zhang

Theoretical analysis and experimental study of vehicle-bridge coupled vibration for highway bridges

Received: 27 March 2023 / Accepted: 20 September 2023 / Published online: 7 November 2023

Abstract Based on the theory of highway vehicle-bridge coupled vibration analysis, a program for vehicle-bridge coupling vibration analysis of highway bridges is developed using Intel Visual Fortran language. An accurate finite element model of the axle was established by measuring the parameters of the axle test model. And an experimental system of vehicle-bridge coupled vibration was designed. Then, based on theoretical analysis and experimental research, the reliability of the analysis program and test system was verified and analyzed the influence factors of vehicle-bridge coupling vibration test were analyzed, including carriageway location, vehicle-bridge mass ratio and bridge support form were discussed. The results show that: a lateral shift of 10 cm at different lane positions has little effect on the dynamic response of the axle. The axle mass ratio is an important factor affecting the dynamic response of the axle. With a vibration response being most obvious when the mass ratio is between 0.10 and 0.16 during the test process, the vertical acceleration response of bridge bearing 1 model (one end pad bearing, the other end roller bearing) was shown to be significant. This research will provide a helpful reference for others to analyze highway vehicle-bridge coupled vibration in the laboratory.

Keywords Highway bridge · Vehicle-bridge coupled vibration · Programming · Experimental study · Numerical simulation

1 Introduction

Vehicle load, as the main load type that the bridge structure, is an important factor affecting the dynamic performance of the bridge. Vehicle driving on the bridge will cause the vibration of the bridge structure, which in turn will affect the safety and stability of the vehicles. The study of the interaction between vehicles and bridges is the category of vehicle-bridge coupling vibration problem, which has become a hot topic in the field of highway bridge research [1–4].

The research methods of vehicle-bridge coupling vibration mainly include theoretical analysis and experimental research. The theoretical analysis methods include: first, the vehicle-bridge coupling vibration differential equation varying with time is derived and solved by taking the vehicle and bridge as a whole and solve it

Z. Li · Z. Li · Y. Zhang (✉) · D. Chen · S. Xu
School of Civil Engineering, Zhengzhou University, Zhengzhou 450001, China
e-mail: m15288279300@163.com

Z. Li
e-mail: lizhengcdh@zzu.edu.cn

Z. Li
e-mail: 18839314553@163.com

Y. Zhang
Henan Transportation Investment Group CO., Ltd., Zhengzhou 450003, China

[5–8]. Second, the vehicle-bridge coupling system is separated into two independent equations of motion, and the two equations of motion are connected through the displacement coordination relationship between the wheel and the bridge floor contact. This method is suitable for the analysis of complex structures or systems with multiple degrees of freedom by combining the finite element method and using analytical calculation for the approximate qualitative analysis of vehicle and bridge models [8–13]. The former has more degrees of freedom, more computation work and more difficulty in solving. The latter adopted the separation iteration method to solve the respective equations of motion, then adopted the geometric equilibrium condition to iterate the respective systems, and finally adopted the time-history analysis method to solve. This method has little workload and easy solution, so it's widely used [14, 15]. Experimental research methods include: one is the real bridge test, the acquisition instrument is placed on the real bridge, collect a lot of data for analysis; the second is the model test. The model bridge is built in the laboratory, and the collection instrument is installed to collect a large number of data for analysis. At present, many test methods adopt the real bridge test, but its cost is high, the test is inconvenient, the test result collection is difficult and the universality is not strong. The model test is easy to operate, good economy, short test cycle and reliable test results.

Tommy [17] made a simple vehicle-bridge coupling vibration model test system, but did not simulate the dynamic characteristics of vehicles and Bridges according to the actual situation, mainly identifying the vehicle-bridge coupling vibration response. Lu [18] made a vehicle-bridge coupling vibration test system and used model tests to verify the correctness of self-excited simulation results. Liu [19] established the vehicle-bridge coupling vibration system of double-tower cable-stayed bridge, which focused on the jump-off impact effect and did not strictly consider the influence of dynamic characteristic parameters on the test. Considering the dynamic characteristics of vehicles and Bridges, Gui [20] made a vehicle-bridge coupling model test system based on 10:1 similarity ratio, taking a three-axle vehicle acting on a 30-m simply supported beam bridge as the prototype, and verified the model test system through numerical simulation.

To sum up, there are some shortcomings in the test verification process of the existing numerical simulation methods of vehicle-bridge coupling vibration of highway Bridges, including: first, the parameters of the vehicle model (such as tire and vibration damping device stiffness and damping coefficient, etc.) are rarely tested, and the dynamic response of the vehicle is difficult to accurately reflect the actual situation in the numerical simulation; secondly, the existing scholars have adopted few model test methods, and there is no unified model test system. Therefore, according to the vehicle-bridge coupling vibration analysis theory of highway bridge, the vehicle-bridge time-varying system is divided into two subsystems: vehicle and bridge. The motion equations of vehicle and bridge subsystems are coupled, and the vehicle-bridge dynamic response is obtained by separation iteration method. Based on the above theory, the process of programming vehicle-bridge coupling vibration analysis program with Intel Visual Fortran language is described. By accurately measuring the model parameters, a test model of bridge and vehicle is made. Then, a set of vehicle-bridge coupling vibration test system is designed, and the influence rule of the test factors such as lane location, vehicle-bridge mass ratio, bridge model support form is discussed. It can provide reference for the laboratory to carry out the experimental study of vehicle-bridge coupling vibration of highway bridge.

2 Analysis method of highway vehicle-bridge coupled vibration

Based on structural dynamics theory, the vehicle and bridge are regarded as two independent subsystems, and their vibration equations are established, respectively. The geometric and mechanical coupled relationship of vehicle-bridge contact points are calculated by iterative ICA (Independent Component Correlation Algorithm) [20–22]. In time-domain, the step-by-step Integration Method is used for solving separately the vibration equations to obtain the vehicle-bridge vibration response [23].

2.1 The motion equation of vehicle

The vehicle is simplified into a multi-rigid space structure consisting of a vehicle body and 4 wheels, and the rigid bodies is connected by springs and damping elements. Three degrees of freedom are considered for the vehicle body, namely, floating and sinking, nodding and lateral rolling, while the wheels only consider floating and sinking and vertical coupling vibration displacement at the contact point with the bridge deck. Namely, the vehicle model has 11 degrees of freedom, as shown in Fig. 1.

Based on the D'Alembert's principle and the static equilibrium position of the vehicle under gravity, the motion equation of the vehicle subsystem can be expressed as follows:

$$M_{\mathrm{v}}\ddot{U}_{\mathrm{v}} + C_{\mathrm{v}}\dot{U}_{\mathrm{v}} + K_{\mathrm{v}}U_{\mathrm{v}} = F_{\mathrm{v}} \tag{1}$$

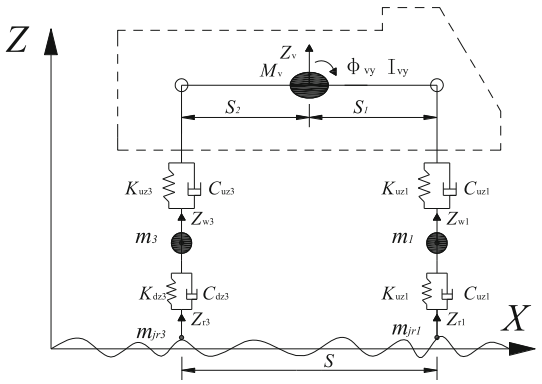

Fig. 1 Vehicle model

where $\ddot{U}_v$, $\dot{U}_v$, and U_v are the global acceleration, velocity and displacement matrices of the vehicle subsystem, respectively; M_v, C_v and K_v are the global mass, damping and stiffness matrices of the vehicle subsystem, respectively; and F_v is the external load matrices of the vehicle subsystem in the vehicle-bridge contact points, which does not consider the gravity of the vehicle.

2.2 The motion equation of bridge

The conventional finite element method is used to simulate the bridge structure. Taking the state without considering the dead weight as the equilibrium position, the motion equation of the bridge subsystem can be expressed as follows:

$$M_b\ddot{U}_b + C_b\dot{U}_b + K_bU_b = F_b \tag{2}$$

where $\ddot{U}_b$, $\dot{U}_b$, and U_b are the global acceleration, velocity and displacement matrices of the bridge subsystem, respectively; M_b, C_b and K_b are the global mass, damping, and stiffness matrices of the bridge subsystem, respectively; and F_b is the external load matrices of the bridge subsystem in the vehicle-bridge contact points, which does consider the gravity of the vehicle.

In practical engineering, the damping mechanism of structure is rather complicated, and the damping coefficient C cannot be accurately calculated. Therefore, Rayleigh damping model is often used to determine the damping ratio. In this paper, the damping ratio is 3%.

2.3 the coupled relationship of vehicle-bridge system

2.3.1 the geometric coupled relationship

At any time when the vehicle is running on the bridge, the wheels are in close contact with the bridge deck and there is no relative displacement. And, the vertical coupled relationship between the vehicle and bridge can be shown in Fig. 2.

$$Z_c = Z_b + r_z \tag{3}$$

The vertical displacement Z_c of vehicle-bridge contact points is equal to the sum of the corresponding bridge displacement Z_b and the road surface roughness r_z at the contact points, which is the geometric coupled relationship of vehicle-bridge coupled vibration.

2.3.2 The mechanical coupled relationship

The connection between the wheel and the bridge is simulated by springs and damping elements, as shown in Fig. 2, the interaction force equation of vehicle-bridge contact points is composed of the elastic force and the damping force, the interaction force can be expressed as follows:

$$F = k_z(Z_w - Z_c) + c_z\left(\dot{Z}_w - \dot{Z}_c\right) \tag{4}$$

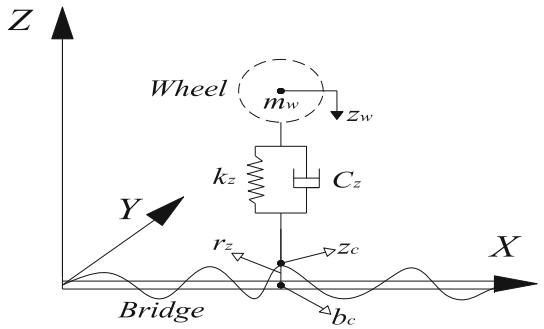

Fig. 2 Vertical coupled relationship of vehicle-bridge system

where F is the interaction force of vehicle-bridge contact points; k_z and c_z are stiffness and damping coefficient of the wheel, respectively; Z_w and $\dot{Z}_w$ are displacement and velocity of the wheel, respectively; Z_c and $\dot{Z}_c$ are displacement and velocity of vehicle-bridge contact points, respectively.

In each time step, F is related to the unknown displacement and velocity of the vehicle and bridge, as shown in Eq. (4). Therefore, iterative computation is needed to solve the interaction force of vehicle-bridge contact points.

Since the motion of the car body and wheels is regarded as a small vibration about the static equilibrium position of the vehicle under gravity, the external load acting on the vehicle is only the interaction force of vehicle-bridge contact points. However, the external load acting on the bridge is vehicle weight and the interaction force of vehicle-bridge contact points.

The elastic damping force of vehicle-bridge contact points is a pair of equal and opposite forces, which reflects the mechanical coupled relationship of vehicle-bridge coupled vibration.

2.4 Equation solving and programming of vehicle-bridge coupled vibration

In each time step, the motion equation of vehicle and bridge is calculated by iterative ICA, and concrete steps can be expressed as follows:

(1) Taking the bridge dynamic response of the previous iterative step as the initial value of the current iteration step, based on the current road surface roughness, the external load of the vehicle subsystem is calculated by Eq. (4);
(2) Based on the Newmark-β method, the vehicle dynamic response of the current iteration step is calculated by Eq. (1);
(3) Calculate the force exerted by each wheel on the bridge (if the elastic and damping force are tensile forces, it means that the wheels are separated from the bridge deck, and the force exerted by the wheels on the bridge is equal to 0) to form the external load matrices of the bridge subsystem;
(4) Based on the Newmark-β method, the bridge dynamic response of the current iteration step is calculated by Eq. (2);
(5) Compare the bridge displacement between the current and the previous iteration to determine the convergence criterion. If the bridge displacement does not converge, repeat steps (1) to (4) until the geometric and mechanical coupled relationship of vehicle and bridge is satisfied; if the bridge displacement converges, start the calculation of the next time step.

Based on the Microsoft Visual Studio 10.0 platform and theory of Highway vehicle-bridge coupled vibration analysis, this paper implements a Fortran-based dynamic analysis program of assembling language. And, the program block diagram is shown in Fig. 3.

In this method, the dynamic responses of the vehicle subsystem and bridge subsystem are solved separately, only the load array of vehicle and bridge is modified in each time step, the mass, damping and stiffness matrix of the system at each time step is avoided, the computation memory is saved and improve the efficiency of calculation. It is convenient for solving complex dynamic problems with a wide range of applications.

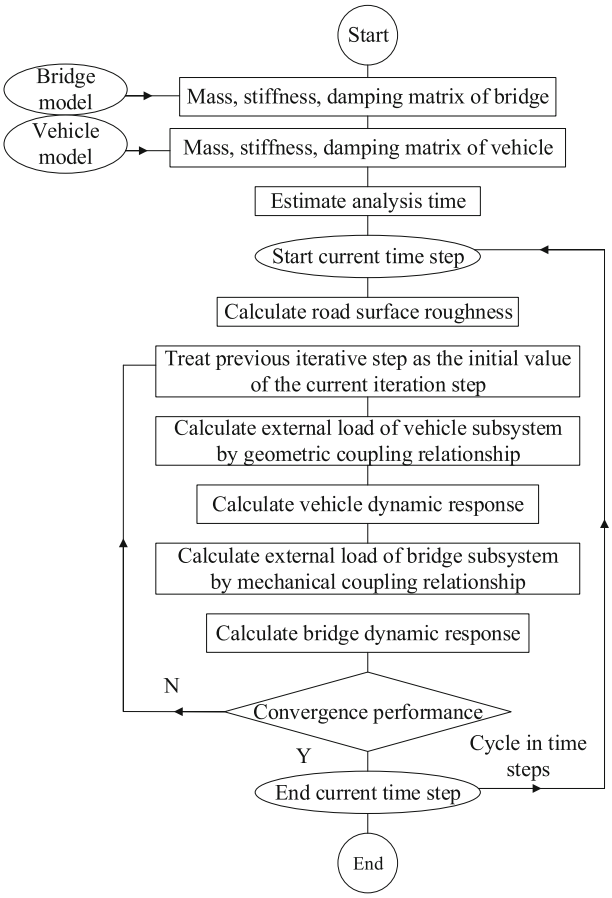

Fig. 3 Dynamic analysis program block diagram

Table 1 Vehicle test model parameters

Positions	Stiffness (N·mm^{-1})	Damping (N·s·m^{-1})
Wheel	96.97	332.40
Front wheel vertical damping spring	14.58	440.91
Rear wheel vertical damping spring	45.65	780.17

3 Experimental study of highway vehicle-bridge coupled vibration

3.1 Vehicle model

The vehicle test model is composed of a frame and rubber wheels with damping springs, as shown in Fig. 4. The frame is welded by steel pipe girder, angle steel tie beam and rectangular cross beams. A motor is installed behind the frame to control the speed of the vehicle, and the test vehicle weighs 45.24 kg.

A spring testing machine (Fig. 5a) is used to test the stiffness coefficient of the vehicle wheel and the damping spring. And through pendulum impact testing machine (Fig. 5b), the damping coefficient of the wheel is calculated by the amplitude of the pendulum and the load applied. The measured parameters of the vehicle test model can be shown in Table 1.

By comparing and analyzing the free vibration experimental and numerical results, error analysis between the two results is used to verify the reliability of the vehicle test model in the experimental model, the fundamental frequency of the vehicle is test by the single point excitation of the force hammer, vibration signals are collected by piezoelectric acceleration sensors (Type INV9818), which are arranged at four corners of the vehicle. The INV3018C signal acquisition and analysis dynamic analyzer were used to collect the vehicle's

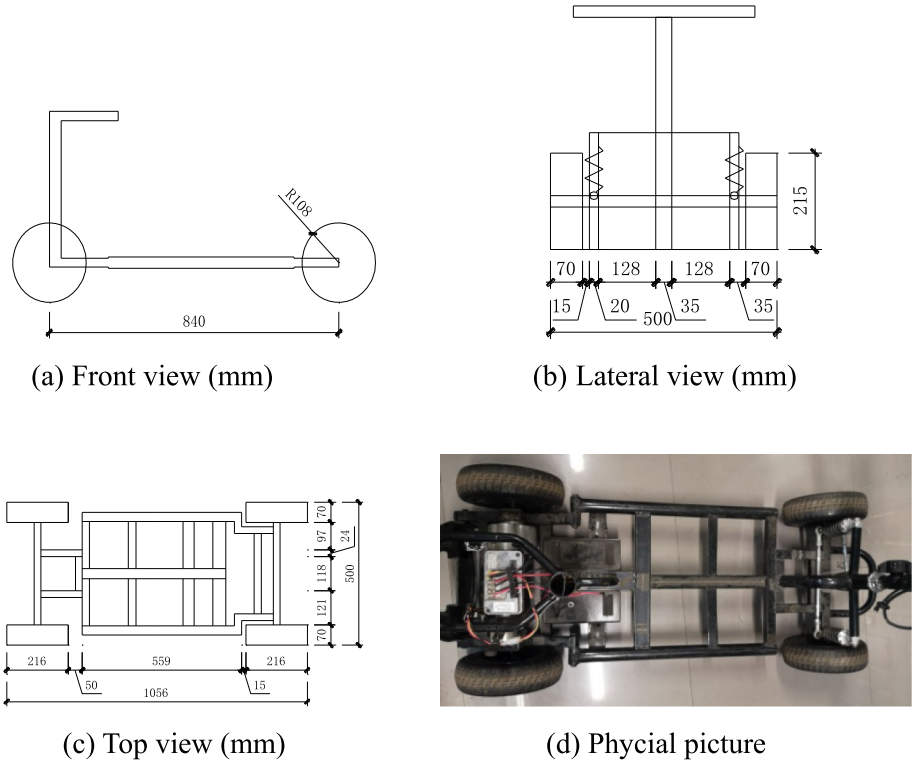

(a) Front view (mm) (b) Lateral view (mm)

(c) Top view (mm) (d) Phycial picture

Fig. 4 Vehicle test model

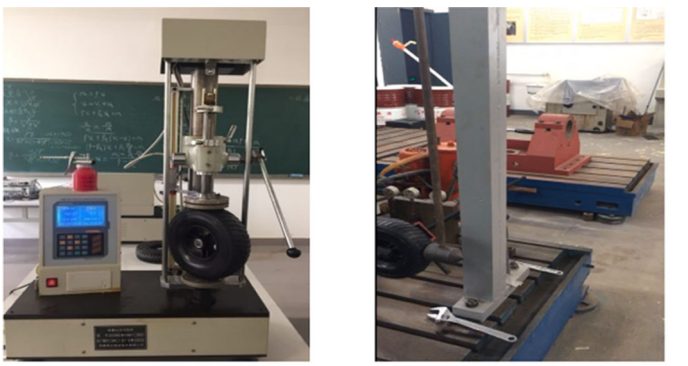

(a) Spring testing machine (b) Pendulum impact testing machine.

Fig. 5 Parameter measuring instrument

free vibration acceleration response, and the DASPV10 dynamic acquisition and analysis system were used to analyze the vehicle's free vibration acceleration signal, and the measured first-order vertical frequency of the vehicle was obtained, as shown in Fig. 6.

In the numerical model, the software ANSYS is applied to set up the finite element model of the vehicle (Fig. 7), The non-load-bearing components which had little influence on the overall structure mass and stiffness distribution were ignored. The Beam189 units were used to simulate the vehicle frame, and the combin14 units with different parameters of the vehicle experimental model in Table 1 were used to simulate the stiffness and damping components of the wheel and the damping spring mass 21 unit simulates the car tire mass, and Beam189 unit simulates the car motor and counterweight with solid circle section. There are 74 nodes and 97 units in the finite element model of the vehicle.

From Fig. 6, the natural vibration frequency of the test vehicle is 19.0 Hz, and the natural vibration frequency calculated by the finite element model is 18.4 Hz, with a difference of 3.16% apart. The experiment value of the fundamental frequency of the vehicle model approximately agrees with the numerical ones, which indicates

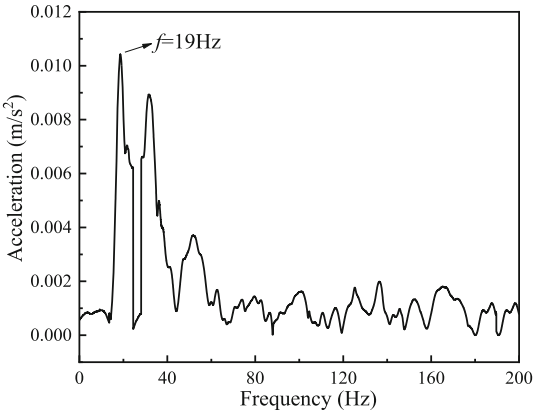

Fig. 6 Fundamental frequency of the vehicle

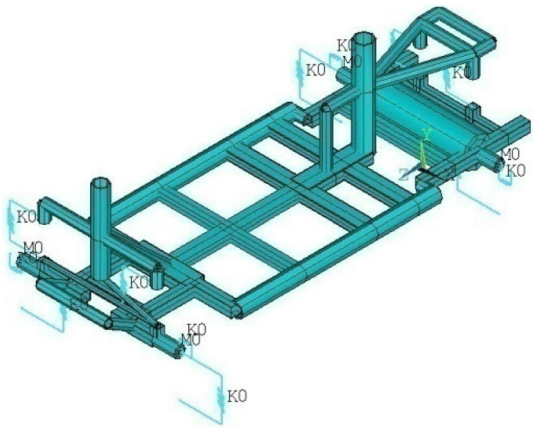

Fig. 7 Vehicle finite element model

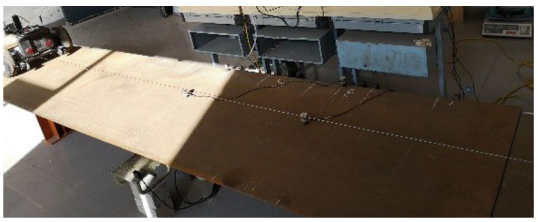

Fig. 8 Bridge test model

that the test and finite element model of vehicle can be used for subsequent vehicle-bridge coupled vibration analysis.

3.2 Bridge model

To amplify the bridge dynamic response, the main girder of the bridge test model selected a steel plate with a smaller stiffness, which is $3 \times 0.8 \times 0.012$ m in size, Q235 of material, and weight of 226.08 kg. The bridge model is divided into 3 spans, with boundary conditions of each one on simply supports, the model1 (pad support at one end and roller support at the other) for a type of support on each one, and 0.1 m distance between support and bridge edge. The mid-span of the bridge is the detection beam, and the two sides are the vehicle acceleration beam and the deceleration beam. The bridge test model is shown in Fig. 8.

By comparing experimental and numerical results of the free vibration and static characteristics, error analysis is used to verify the reliability of the bridge test model. In the static experiment, a 12kg counterweight

Table 2 Vertical displacement at measuring point

Measurement times	Vertical displacement (mm)
The first time	2.559
The second time	2.568
The third time	2.575
Average value	2.567

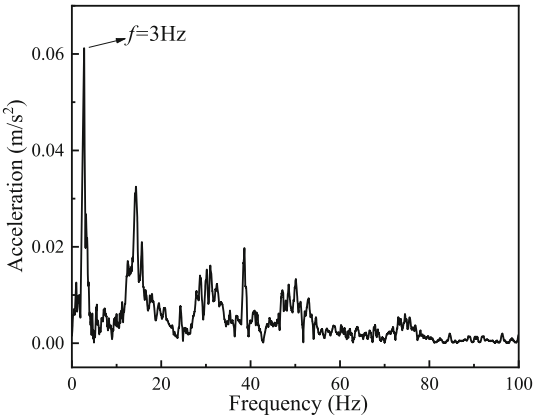

Fig. 9 Fundamental frequency of the bridge

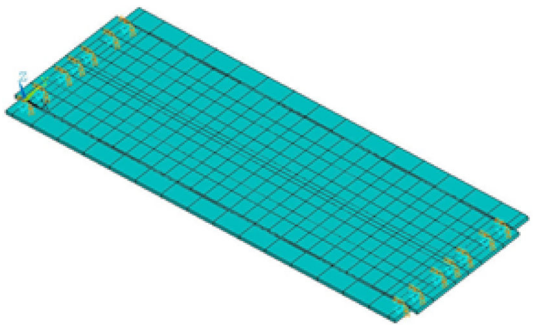

Fig. 10 Bridge FE mode

Table 3 Numerical and experimental comparison of bridge model

Item	Experimental value	Numerical value	Difference/%
Deflection of bridge mid-span (mm)	2.567	2.451	4.52
Fundamental frequency (Hz)	3.000	3.1343	4.28

was piled up in the mid-span of the bridge test model, and a dial indicator was used to measure the mid-span deflection, as shown in Table 2. The fundamental frequency of the bridge is tested by a single point excitation method. The bridge vibrates freely by hammering with a rubber force hammer. The vibration signal is collected by a piezoelectric acceleration sensor (model INV9818). The frequency spectrum of the bridge's free vibration acceleration is analyzed to obtain the first-order vertical natural vibration frequency of the bridge, as shown in Fig. 9.

The software ANSYS is applied to set up the finite element model of the bridge (Fig. 10) by grillage method [24], with a BEAM44-element-based bridge structure. The length of the bridge model is $l = 3$ m, and the material is Q235 steel. The simple support constraint is adopted at both ends of the support, there are 126 nodes and 215 unites in total. A nodal force $F = 120$ N is applied to the mid-span of the model to obtain the displacement. The vertical frequency can be calculated by finite element software. The comparison between measured and theoretical values of vertical deflection and vertical frequency in the span is shown in Table 3.

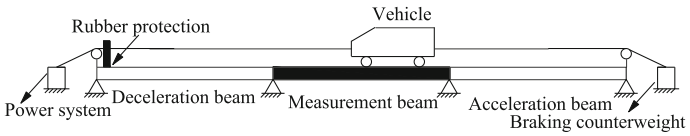

Fig. 11 Experimental system of vehicle-bridge coupled vibration

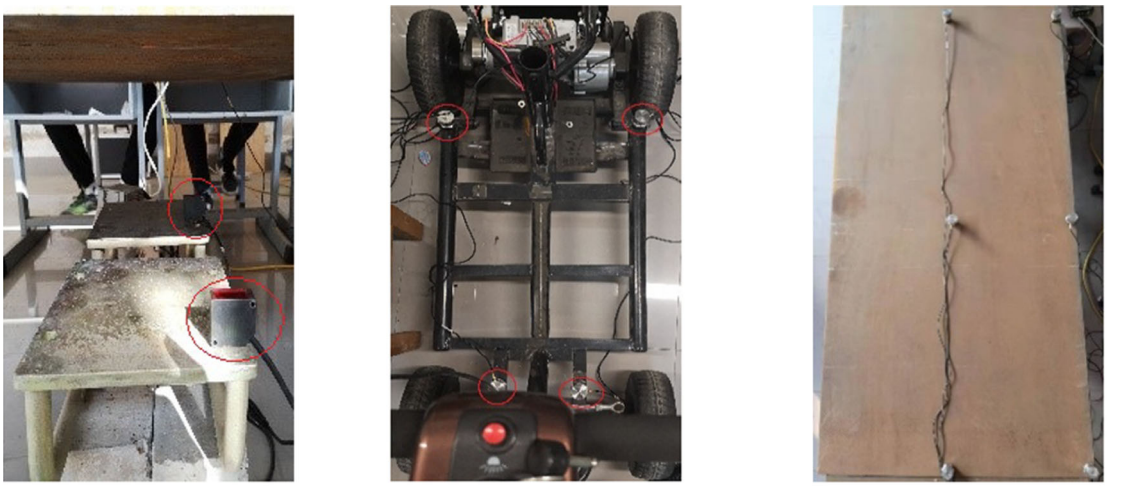

(a) Laser displacement sensors, (b) Piezoelectric accelerometers of vehicle (c) Piezoelectric accelerometers of bridge.

Fig. 12 Measuring points layout

Table 3 shows that the experimental value of the fundamental frequency and mid-span deflection of the bridge model approximately agrees with the numerical one, in which the differences are all less than 5%. And it indicates that the test and finite element model of bridge can be used for subsequent vehicle-bridge coupled vibration analysis.

3.3 Experimental system of vehicle-bridge coupled vibration

The experimental system of vehicle-bridge coupled vibration is composed of a vehicle-bridge test model and an experimental power system. The experimental power system includes a motor drive system and a braking device; the bridge test model is divided into an acceleration beam, a measurement beam and a deceleration beam.

In the experiment, the motor drive system controls the wire rope to pull the vehicle through a fixed pulley to accelerate from a standstill to a set speed in the acceleration beam, then pass the measuring beam at a constant speed, and finally brake on the deceleration beam. To ensure the final braking of the vehicle, a rubber protective device is installed at the end of the deceleration beam, and a braking counterweight device is connected to the rear of the vehicle. The experimental system of vehicle-bridge coupled vibration is shown in Fig. 11.

4 Comparative analysis of numerical and experimental model

Based on the experimental system of vehicle-bridge coupled vibration, the driving experiments were carried out on the middle lane of the bridge. Three situations were set up in which the vehicle passed through the bridge measuring beam with the vehicle speed of 0.5 m/s, 1.0 m/s, and 1.5 m/s, respectively.

Two laser displacement sensors are placed under the bridge mid-span to measure the displacement time histories, and the piezoelectric accelerometers are evenly distributed in the bridge deck and vehicle to measure the acceleration response of the vehicle and bridge mid-span, as shown Fig. 12.

Then, in finite element model of the bridge and vehicle, the dynamic response of the vehicle and bridge under the same conditions as that in the driving experiments is calculated by dynamic analysis program of vehicle-bridge coupled vibration.

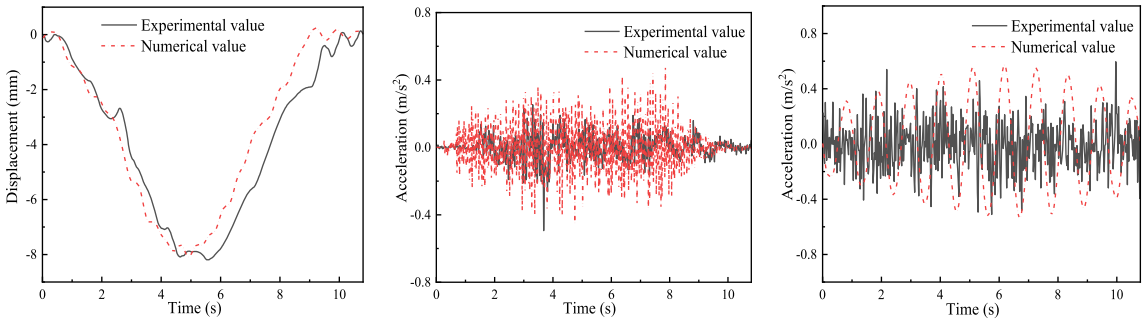

(a) Vertical displacement time history curve of bridge mid-span

(b) Vertical acceleration time history curve of bridge mid-span

(c) Vertical acceleration time history curve of vehicle

Fig. 13 Dynamic response of vehicle-bridge coupled vibration

Table 4 Responses peak of vehicle-bridge coupled vibration

Vehicle speed (m s^{-1})	0.5	1.0	1.5
Vertical displacement of bridge mid-span			
Experimental value (mm)	8.194	8.437	9.037
Numerical value (mm)	8.095	8.183	8.517
Difference/%	1.223	3.104	6.105
Vertical acceleration of bridge mid-span			
Experimental value ($m{\cdot}s^{-2}$)	0.494	1.183	1.356
Numerical value ($m{\cdot}s^{-2}$)	0.478	1.152	1.323
Difference/%	3.347	2.691	2.494
Vertical acceleration of vehicle			
Experimental value ($m{\cdot}s^{-2}$)	0.596	0.681	0.797
Numerical value ($m{\cdot}s^{-2}$)	0.572	0.656	0.763
Difference/%	4.20%	3.81%	4.46%

Table 5 Conditions in mass ratio of bridge and vehicle

Conditions	1	2	3	4	5
Vehicle weight (kg)	26.04	35.64	45.24	54.84	64.44
Mass ratio (λ)	0.115	0.158	0.200	0.243	0.285

With the vehicle speed of 0.5 m/s, the experimental and numerical values of vertical displacement and acceleration time history curve of bridge mid-span, and vertical acceleration time history curve of vehicle can be shown in Fig. 13 and the dynamic response peak of each condition can be shown in Table 4.

Figure 13 shows that the experimental value of vehicle-bridge dynamic response approximately agrees with the numerical ones, and the dynamic response curve of vehicle and bridge conforms to the law of vehicle-bridge coupled vibration. Table 3 shows that with the increase in vehicle speed, the dynamic response of vehicle and bridge increases, and the experimental and numerical dynamic response peak of vehicle and bridge have high consistency, and most values of the relative differences are less than 5%. The feasibility of the vehicle-bridge coupled vibration experiment and the reliability of numerical analysis model are verified.

5 Parameter analysis of vehicle-bridge coupled vibration experiment

5.1 Mass ratio of bridge and vehicle

With the bridge weight of 226.08 kg, the mass ratio of bridge and vehicle is set by applying counter weight on the test vehicle, and the setting of mass ratio is shown in Table 5. The speed of the test vehicle is 1.0 m/s.

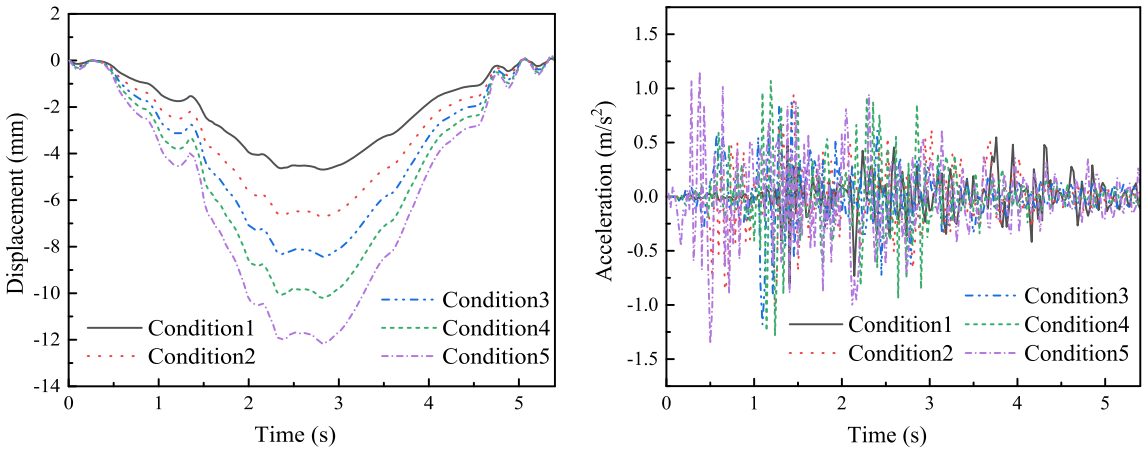

(a) Vertical displacement time history curve (b) Vertical acceleration time history curve

Fig. 14 Dynamic responses of bridge mid-span

Table 6 Vertical responses peaks of bridge mid-span in each condition

Conditions	1	2	3	4	5
Displacement (mm)	4.693	6.720	8.437	10.20	12.16
$\frac{l_i - l_{i-1}}{l_{i-1}}\%$	0	43.19	25.55	20.92	19.16
Acceleration (m·s^{-2})	0.802	1.063	1.183	1.284	1.357
$\frac{\ddot{U}_{bi} - \ddot{U}_{bi-1}}{\ddot{U}_{bi-1}}\%$	0	32.54	11.29	8.54	5.69
$\frac{\lambda_i - \lambda_{i-1}}{\lambda_{i-1}}\%$	0	37.39	26.58	21.50	17.28

l_i indicates displacement of bridge mid-span, $\ddot{U}_{bi}$ indicates acceleration of bridge mid-span, and λ_i indicates mass ratio of bridge and vehicle (i is the condition number, $i = 1, 2, 3, 4, 5$)

5.1.1 Influence of mass ratio on bridge dynamic response

By measuring the dynamic responses of bridge with different mass ratios, the time history curves of vertical displacement and acceleration of the bridge mid-span can be shown in Fig. 14, with the vehicle speed of 1.0 m/s. And, the comparison of the dynamic response peak is shown in Table 6.

Figure 14 shows that with the increase in the mass ratio, the dynamic response of the bridge increases significantly, and the vibration of the bridge is more likely to be excited by heavy vehicles. However, the vibration trend of the bridge mid-span caused by different vehicle weights is roughly the same. Table 6 shows that with the increase in the mass ratio, the responses peak of vertical displacement and acceleration in the bridge mid-span gradually increases. When the mass ratio increases from 0.115 to 0.285, the vertical displacement peak increases from 4.693 to 12.16 mm, and the vertical acceleration peak increases from 0.802 to 1.357 m/s^2. The vertical displacement peak in the bridge mid-span increases approximately in equal proportion with the mass ratio. When the mass ratio is less than 0.16, the vertical acceleration peak in the bridge mid-span increases greatly, and then gradually slows down.

5.1.2 Influence of mass ratio on vehicle dynamic response

By measuring the dynamic response of vehicle with different weights, the time history curves of vertical acceleration can be shown in Fig. 15, with the vehicle speed of 1.0 m/s. And, the comparison of peak of the dynamic response is shown in Table 7.

Figure 15 and Table 7 show that the vertical acceleration peak of vehicle decreases with the increase in mass ratio of vehicle and bridge. When the mass ratio increases from 0.115 to 0.158, the peak vertical acceleration of vehicle decreases by 37.41%. The results show that the vibration amplitude of vehicle decreases with the increase in the vehicle weight.

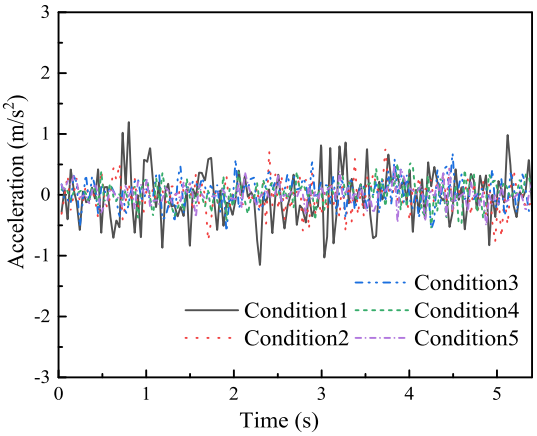

Vertical acceleration time history curve

Fig. 15 Dynamic responses of vehicle

Table 7 Vertical responses peaks of vehicle in each condition

Conditions	1	2	3	4	5
Acceleration ($m \cdot s^{-2}$)	1.195	0.748	0.681	0.553	0.503
$\frac{\ddot{U}_{vi}-\ddot{U}_{vi-1}}{\ddot{U}_{vi-1}}$%	0	− 37.41	− 8.96	− 18.80	− 9.04

$\ddot{U}_{vi}$ indicates vertical acceleration of vehicle and λ_i indicates mass ratio of bridge and vehicle (i is the condition number, $i = 1$, 2, 3, 4, 5)

Table 8 Peak vertical responses of bridge mid-span in different lanes

Vehicle speed ($m \cdot s^{-1}$)	Vertical response peak	Left lane	Middle lane	Right lane
1.0	Displacement (mm)	9.124	8.437	8.803
	Acceleration ($m \cdot s^{-2}$)	1.250	1.183	1.222

In summary, the mass ratio is an important factor affecting the dynamic responses of vehicle-bridge coupled vibration. In an experiment, to obtain obvious dynamic response of bridge and vehicle, it is suggested that the selection range of mass ratio is 0.10~0.16.

5.2 Lane positions

Selecting the test vehicle with a weight of 45.24 kg, the dynamic responses of vehicle-bridge coupled vibration under different lanes was calculated. The left and right lanes move outward by 10 cm compared with the middle lane, and the lane layout is shown in Fig. 16.

5.2.1 Influence of lane positions on bridge dynamic response

By measuring the dynamic responses of bridge, the time history curves of vertical displacement and acceleration of the bridge mid-span can be shown in Fig. 17, with the vehicle speed of 1.0 m/s. And, the comparison of the dynamic response peak is shown in Table 8.

Figure 17 and Table 8 show that the vertical displacement and acceleration responses of the left and right lanes are greater than those of the middle lane, and the left lane has the largest response. This is because when the vehicle is driving in the left or right lane, one side of the wheel is close to the measuring point of the central axis, which increases the deflection of bridge. This shows that the torsional displacement of bridge caused by the eccentric load is less than that caused by vertical force.

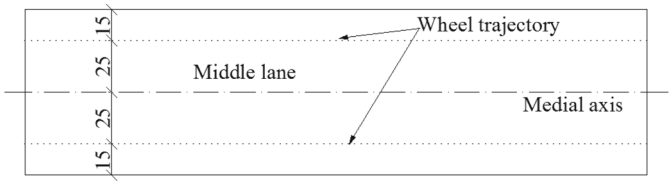

(a) Middle lane

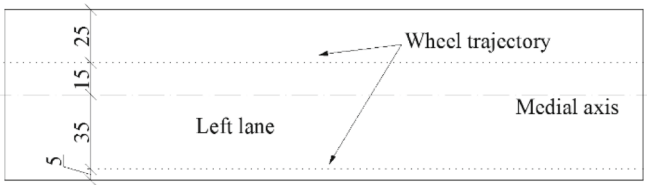

(b) Left lane

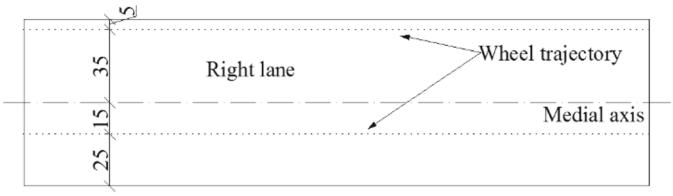

(c) Right lane

Fig. 16 Lane position layout (cm)

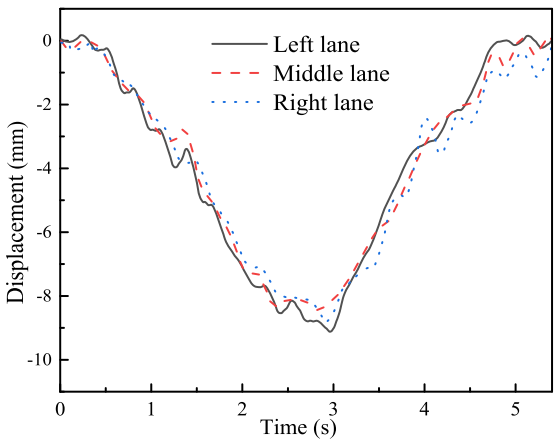

(a) Vertical displacement time history curve

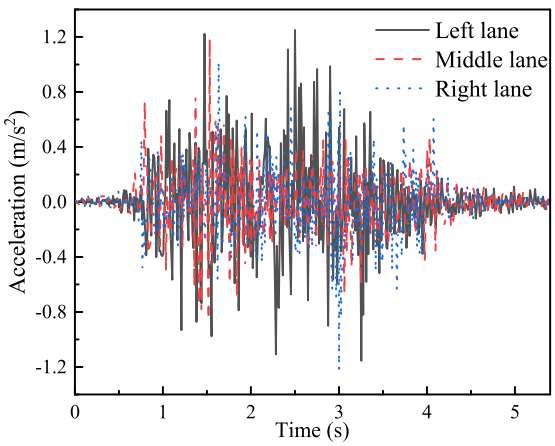

(b) Vertical acceleration time history curve

Fig. 17 Dynamic responses of bridge mid-span

Table 9 Vertical responses peak of vehicle in each condition

Vehicle speed ($m \cdot s^{-1}$)	Response peak	Left lane	Middle lane	Right lane
1.0	Acceleration ($m \cdot s^{-2}$)	0.749	0.681	0.717

5.2.2 Influence of lane position on vehicle dynamic response

By measuring the dynamic response of vehicle in different lanes, the time history curves of vertical acceleration can be shown in Fig. 18, with the vehicle speed of 1.0 m/s. And, the comparison of peak of the dynamic response is shown in Table 9.

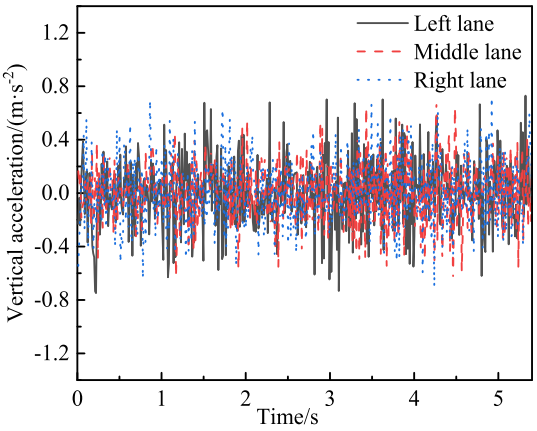

Vertical acceleration time history curve

Fig. 18 Dynamic responses of vehicle

(a)Roller support (b) Pad support (c) Plate support

Fig. 19 Bridge support forms

Table 10 Responses peaks of bridge mid-span in each condition

Vehicle speed (m·s^{-1})	Vertical response peak	Model 1	Model 2	Model 3
1.0	Displacement (mm)	8.437	8.316	6.536
	Acceleration (m·s^{-2})	1.183	1.239	1.367

Figure 18 and Table 9 show that the responses of vehicle-bridge coupled vibration in the middle lane is the minimum than other lines, and the results show that different lanes have little influence on the dynamic response of vehicle and bridge, and the lanes can be selected according to actual needs in the experiment.

5.3 Bridge support forms

Three kinds of bridge support forms (Fig. 19) commonly used in the experiment are selected to analysis vehicle-bridge coupled vibration. These bridge support forms are combined into three kinds of support models, in which model 1 is pad support at one end and roller support at the other; model 2 is pad support at both ends; model 3 is plate support at both ends. Selecting the test vehicle with a weight of 45.24 kg, the vehicle runs in the middle lane of different bridge support model.

5.3.1 Influence of support forms on bridge dynamic response

By measuring the dynamic responses of bridge with different support models, the time history curves of vertical displacement and acceleration of the bridge mid-span can be shown in Fig. 20 with the vehicle speed of 1.0 m/s. And, the comparison of the dynamic response peak is shown in Table 10.

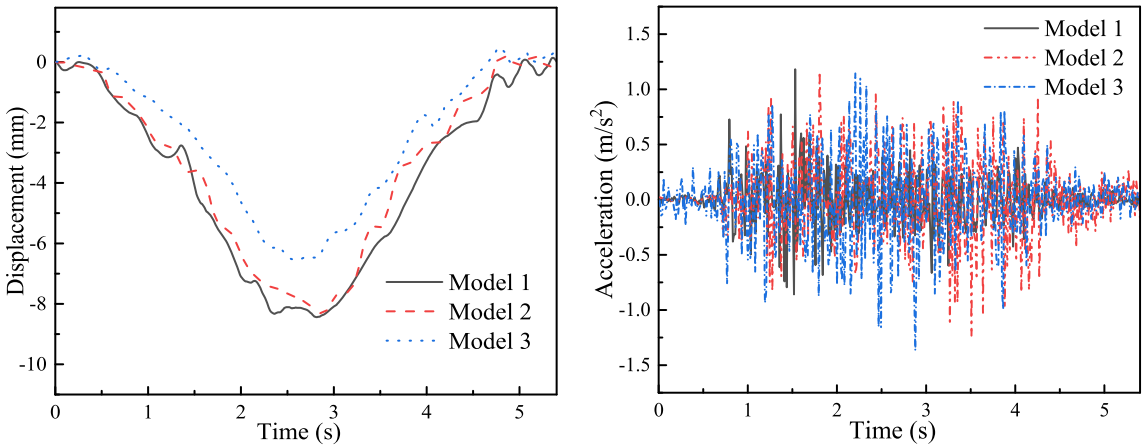

(a) Vertical displacement time history curve (b) Vertical acceleration time history curve

Fig. 20 Dynamic responses of bridge mid-span

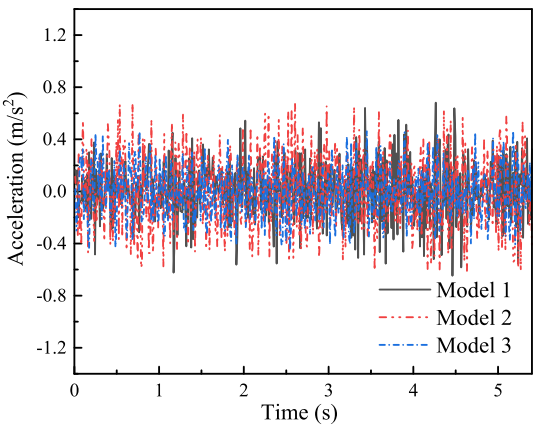

Vertical acceleration time history curve

Fig. 21 Dynamic responses of vehicle

Table 11 Vertical responses peak of vehicle in each condition

Vehicle speed ($m \cdot s^{-1}$)	Response peak	Model 1	Model 2	Model 3
1.0	Acceleration ($m \cdot s^{-2}$)	0.681	0.678	0.472

Figure 20 and Table 10 show that with the same of vehicle speed, the vertical displacement peak in the bridge mid-span under model 3 is the smallest, which is reduced by 22.5% compared with model 1. However, the vertical acceleration peak in the bridge mid-span is the largest, which is increased by 15.6% compared with model 1.

5.3.2 Influence of support forms on vehicle dynamic response

By measuring the dynamic response of vehicle under different support models, the time history curves of vertical acceleration can be shown in Fig. 21, with the vehicle speed of 1.0 m/s. And, the comparison of peak of the dynamic response is shown in Table 11.

Figure 21 and Table 11 show that, with the same of vehicle speed, the vertical acceleration of vehicle under the model 3 is the smallest, which peak is reduced by 30.69% compared with the model 1.

In summary, the support forms have an obvious influence on the dynamic response of vehicle-bridge coupled vibration. To obtain significant dynamic responses of vehicle and bridge, the model 1 should be selected for the bridge support in the experiment.

6 Conclusion

(1) Based on the theory of vehicle-bridge coupled vibration analysis of highway bridges, this paper implements a Fortran-based dynamic analysis program of assembling language, designs an experimental system of vehicle-bridge coupled vibration. The system can simulate the uniform motion of vehicle when passing through the bridge by measuring accurate vehicle parameters.
(2) The experimental value of the fundamental frequency and dynamic responses of the vehicle and bridge model approximately agrees with the numerical ones, which verifies the feasibility of the experimental system and the reliability of the dynamic analysis program.
(3) In the experiment, the vehicle-bridge coupled vibration response in the middle lane is the minimum than other lanes, and it presents a monotonous increasing trend with the increase in vehicle speed. The side shift of 10 cm lane position has little influence on the dynamic response of vehicle and bridge, so the lane can be selected according to the actual needs.
(4) The mass ratio of vehicle and bridge is an important factor affecting the dynamic response of vehicle-bridge coupled vibration. To obtain obvious vibration response of bridge and vehicle in the experiment, it is suggested that the selection range of mass ratio is 0.10–0.16.
(5) The bridge support forms have an obvious influence on the dynamic response of vehicle-bridge coupled vibration. To obtain obvious vehicle and bridge vibration response in the experiment, the support forms can choose the model 1.

Acknowledgements The study was supported by the National Natural Science Foundation of China (No. 51408557), China Postdoctoral Science Foundation (No. 2013M541995), and Henan Province Department of Transportation (No. 2020J-2-6).

References

1. Coutinho, C.P., Baptista, A.J., Rodrigues, J.D.: Reduced scale models based on similitude theory: a review up to 2015. Eng. Struct. **119**, 81–94 (2016). https://doi.org/10.1016/j.engstruct.2016.04.016
2. Deng, L., He, W., Yu, Y., Wang, W.: Research progress in theory and applications of highway vehicle-bridge coupled vibration. China. J. Highw. Transp. **31**, 38–54 (2018)
3. Zhai, W.M., Han, Z.L., Chen, Z.W., Ling, L., Zhu, S.Y.: Train-track-bridge dynamic interaction: a state-of-the-art review. Veh. Syst. Dyn. **57**, 984–1027 (2019). https://doi.org/10.1080/00423114.2019.1605085
4. Deng, L., Yu, Y., Zou, Q.L., Cai, C.S.: State-of-the-art review of dynamic impact factors of highway bridges. J. Bridge. Eng. (2015). https://doi.org/10.1061/(ASCE)BE.1943-5592.0000672
5. Stoke, G.G.: Discussions of a differential equation related to the breaking of railing of railway bridges. Trans. Camb. Philos. Soc. V **8**(Part 5), 12–16 (1896)
6. Chatterjee, P.K., Datta, T.K., et al.: Vibration of continues bridges under moving vehicles. J. Sound Vib. **169**(5), 619–632 (1994)
7. Kolousek, V. et al.: Civil Engineering Structures Subjected to Dynamic Load, pp. 54–58. SVTL, Bratislava (1967)
8. Andersen, L., Nielsen, S.R.K., Iwankiewicz, R.: Vehicle moving along an infinite beam with random surface irregularities on a Kelvin foundation. J. Appl. Mech. **66**, 69–75 (2002). https://doi.org/10.1115/1.1427339
9. Kawatani, M., Kobayashi, Y., Takamori, K.: Non-stationary random analysis with coupling vibration of bending and torsion of simple girder-bridge under moving vehicle. Struct. Eng. Earthq. Eng. JSCE **15**(1), 107–114 (1998)
10. Marchesiello, S., Fasana, A., Garibaldi, L., et al.: Dynamic of multi-span continuous straight bridges subject to multi-degrees of freedom moving vehicle excitation. J. Sound Vib. **224**(3), 541–561 (1999). https://doi.org/10.1006/jsvi.1999.2197
11. Wang, T.L., Huang, D.Z.: Cable-stayed bridge vibration due to road surface roughness. J. Struct. Eng. **188**(5), 1354–1373 (1992)
12. Schelling, D.R., Galdos, N.H., Sahin, M.A.: Evaluation of impact factors for horuzontally curved steel box bridges. J. Struct. Eng. **118**(11), 3203–3221 (1992)
13. Galdos, N.H., Schelling, D.R., Sahin, M.A.: Methodology for impact factors of horuzontally curved box bridges. J. Struct. Eng. **119**(6), 1917–1934 (1993)
14. Chu, K.H., Grag, V.K., Dhar, C.L.: Railway bridge impact, simplified train and bridge mode. J. Struct. Div. **105**(ST9), 1823–1844 (1979)
15. Li, X.: Theory and Application of Space-Coupled Vibration of High-Speed Railway Train-Bridge System. Doctoral dissertation. Southwest Jiaotong University, Chengdu (20000
16. Shen, R.: Research on Coupled Vibration of High-Speed Railway Bridge and Vehicle. Doctoral dissertation. Southwest Jiaotong University, Chengdu (1998)

17. Chan, T.H.T., Ashebo, D.B.: Moving axle load from multi-span continuous bridge: laboratory study. J. Vib. Acoust. **128**, 521–526 (2006). https://doi.org/10.1115/1.2202154
18. Lu, K., Qiu, H.: Coupled vibration analysis of container trolley-low bridge structure under wind and earthquake loads. Eng. Mech. **29**(10), 313–320 (2012)
19. Xijun, L., Linjie, X., Suxia, Z., et al.: Vibration impact of derailment on bridge based on wavelet analysis. J. Vib. Meas. Diagnos. **35**(06), 1123–1128 (2015)
20. Gui, S., Chen, S., Wan, S.: Experimental design and verification of vehicle-bridge coupled vibration model for highway bridges. J. Jiangsu Univ. Nat. Sci. Ed. **35**(04), 463–469 (2014)
21. Guebailia, M., Ouelaa, N., Guyader, J.L.: Solution of the free vibration equation of a multi span bridge deck by local estimation method. Eng. Struct. **48**, 695–703 (2013). https://doi.org/10.1016/j.engstruct.2012.12.004
22. Zhang, N., Xia, H.: Dynamic analysis of coupled vehicle-bridge system based on inter-system iteration method. Comput. Struct. **114**, 26–34 (2013)
23. Krishnanunni, C.G., Rao, B.N.: Decoupled technique for dynamic response of vehicle-pavement systems. Eng. Struct. **191**, 264–279 (2019). https://doi.org/10.1016/j.engstruct.2019.04.042
24. Han, W.S., Wang, T., Li, Y.Q., Li, Y.W., Huang, P.M.: Analysis system of vehicle-bridge coupled vibration with grillage method based on model updating. China. J. Highw. Transp. **24**, 47–55 (2011)